

Enhanced Polymeric Dielectrics through Incorporation of Hydroxyl Groups

Mayank Misra,[†] Manish Agarwal,[†] Daniel W. Sinkovits,[†] Sanat K. Kumar,^{*,†} Chenchen Wang,[‡] Ghanshyam Pilania,[‡] Ramamurthy Ramprasad,[‡] Robert A. Weiss,[§] Xuepei Yuan,^{||} and T. C. Mike Chung^{||}

[†]Department of Chemical Engineering, Columbia University, 500 West 120th Street, New York, New York 10027

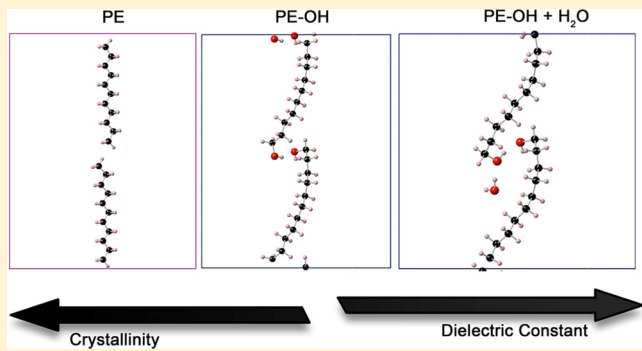
[‡]Department of Chemical, Materials and Biomolecular Engineering and Institute of Material Science, University of Connecticut, Storrs, Connecticut 06269-3136

[§]Department of Polymer Engineering, University of Akron, Akron, Ohio 44325

^{||}Department of Materials Science and Engineering, The Pennsylvania State University, University Park, Pennsylvania 16802

S Supporting Information

ABSTRACT: We use simulations and experiments to delineate the mechanism by which the addition of a small number of polar $-\text{OH}$ groups to a nonpolar polymer increases the static relative permittivity (or dielectric constant) by a factor of 2, but more importantly while keeping the dielectric loss in the frequency regime of interest to power electronics to less than 1%. Dielectric properties obtained from experiments on functionalized polyethylenes and polypropylenes as a function of $-\text{OH}$ doping are in quantitative agreement with one another. Molecular dynamics simulations for the static relative permittivity of “dry” $-\text{OH}$ functionalized polyethylene (in the absence of water) are apparently in quantitative agreement with experiments. However, these simulation results would further imply that there should be considerable dielectric loss beyond simulation time scales ($>0.1\ \mu\text{s}$). Since there are minimal experimentally observed dielectric losses for times as short as a microsecond, we believe that a small amount of adsorbed water plays a critical role in this attenuated loss. We use simulations to derive the water concentration at saturation, and our results for this quantity are also in good agreement with experiments. Simulations of the static relative permittivity of PE–OH incorporating this quantity of hydration water are found to be in quantitative agreement with experiments when it is assumed that all the dipolar relaxations occur at time scales faster than $0.1\ \mu\text{s}$. These results suggest that improved polymeric dielectric materials can be designed by including $-\text{OH}$ groups on the chain, but the mechanism requires the presence of a stoichiometric quantity of hydration water.



1. INTRODUCTION

The demand for capacitor dielectrics in power electronics for high voltage pulse generations is increasing in various technological sectors such as hybrid vehicles, food preservation and the defense industry. Metallized polymer films have significant advantage over ceramic capacitors in this context due to their ease of processability, low weight and self-healing ability.¹ The state of the art in polymeric capacitor films is metallized biaxially oriented polypropylene (BOPP), with an energy storage density of $\sim 2.2\ \text{J}/\text{cm}^3$.^{2,3} Metallized BOPP has the unique combination of fast response, low loss, and high breakdown field in the range of $700\ \text{V}/\mu\text{m}$ for small areas. Any improvement to polypropylene (PP) would require an increase in relative permittivity and/or breakdown strength while preserving low loss. While the obvious strategy of adding polarizable groups to PP does increase its relative permittivity, the slowed-down dynamics of most polar groups also produces increased dielectric loss in the range of frequencies relevant to

power electronics. The improvement of the dielectric properties of PP has thus remained an open challenge in this field.

Recent experimental studies indicate that the covalent addition of a small amount (2–6 mol %) of $-\text{OH}$ groups to isotactic PP chains alleviates these difficulties. Indeed, it was found that the addition of these hydroxyl groups causes a significant increase in the static relative permittivity of the polymer while still maintaining a relatively low dielectric loss.⁴ While the origins of these results have been attributed to the high crystallinity of PP coupled to a unique hydrogen bonding network structure caused by the $-\text{OH}$ groups, little molecular understanding exists of these unusual phenomena. Probing these molecular processes through the aid of large-scale molecular dynamics simulations, in

Received: October 26, 2013

Revised: December 9, 2013

Published: January 29, 2014

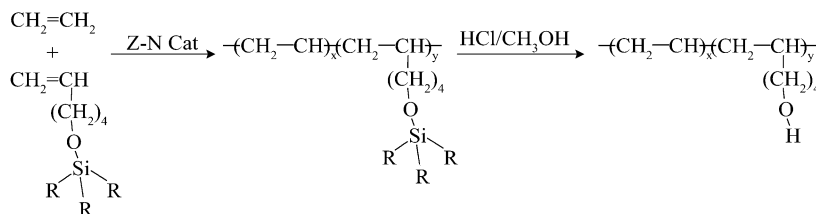


Figure 1. Scheme for synthesis of copolymer PE–OH.

conjunction with experimental findings, is the primary focus of this contribution.

While the crystallization of PP is hard to simulate,⁵ polyethylene (PE) crystallizes readily even during typical MD simulations.^{6–12} So, from a simulation point of view, it makes sense to focus on copolymers of PE. We are further guided to this choice since experimental dielectric storage and loss results for PP–OH and new results for PE–OH both behave similarly (see below). These support the generality of our assertion that the addition of –OH groups to a nonpolar hydrocarbon chain serves to increase its static relative permittivity without simultaneously increasing loss.

We begin by discussing the two relevant set of experiments, and follow up with our simulations. We simulate dry PE–OH and find that the incorporation of the polar hydroxyl groups does serve to increase the static relative permittivity. However, a more detailed analysis shows that there must be a slower time scale process, which should yield considerable dielectric loss over experimentally relevant frequencies. Since the experiments yield no such increased loss, we conjecture that some other factor is relevant. Indeed, we find both from experiments and simulations that the PE–OH chains have a small amount of hydration water associated with them. Simulations of PE–OH with its hydration water, and the comparison of these simulations to experiments, allow us to conclude that the water-mediated hydrogen bonding of the –OH groups to each other results in only fast relaxations, well beyond the frequencies typically used in power electronics (1 MHz). It is thus apparent that the presence of water and the –OH groups, in conjunction, are critically important for the dual phenomena of increased dielectric storage while maintaining low loss.

2. EXPERIMENTS

2.1. Synthesis. For the experimental investigation of the dielectric properties of PE, we synthesized random copolymers of ethylene and vinyl groups with a hydrocarbon side chain terminated with an –OH group (Figure 1). We copolymerize ethylene and a comonomer containing silane using Ziegler–Natta catalysis. Following this, we interconvert the resulting silane-containing PE copolymer into the copolymer PE–OH; further details are provided in the Supporting Information. Figure 2 shows the ¹H NMR spectra of a 5.9 mol % of PE copolymer which proves the successful synthesis of the copolymer PE–OH.

2.2. Film Processing and Dielectric Characterization. Vacuum-melting pressing was performed at the optimized temperature and pressure (220 °C and 24000 psi for PE) with the samples placed between Teflon sheets for the preparation of films of thickness around 50 μm, which were subsequently annealed in a vacuum oven at 90 °C for 8 h. Higher temperatures were avoided because that causes the film to wrinkle and shrink, thereby damaging the sample. The polymer film was then sputtered with gold (<0.1 μm thickness) on both surfaces. The

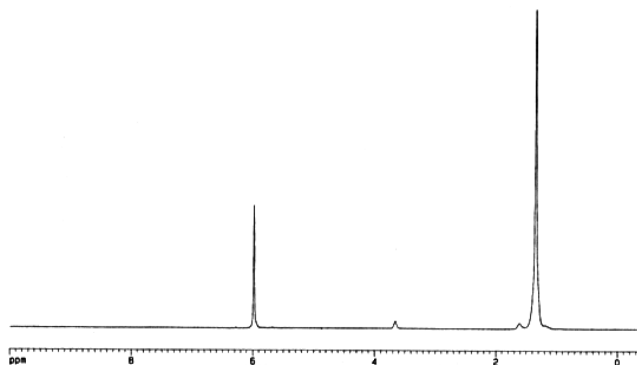


Figure 2. ¹H NMR spectra of PE-7 ([–OH] = 5.90 mol %). The peak at 1.30 ppm is typical of methylene hydrogens. The small peaks at 3.6 and 1.5 ppm are ascribed to the hydrogens of the methylene groups in the spacers nearest and next-nearest to the –OH group.

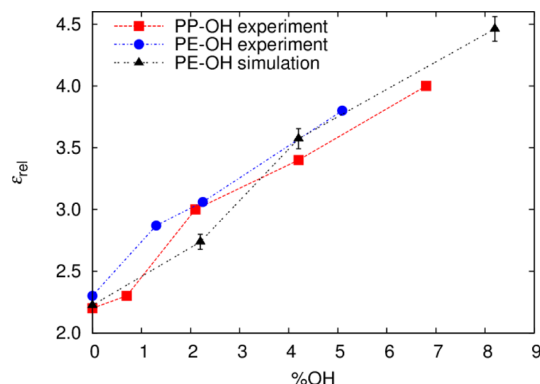


Figure 3. Static relative permittivity, ϵ_{rel} , comparison of PP–OH and PE–OH. The simulation values are derived as discussed in the text.

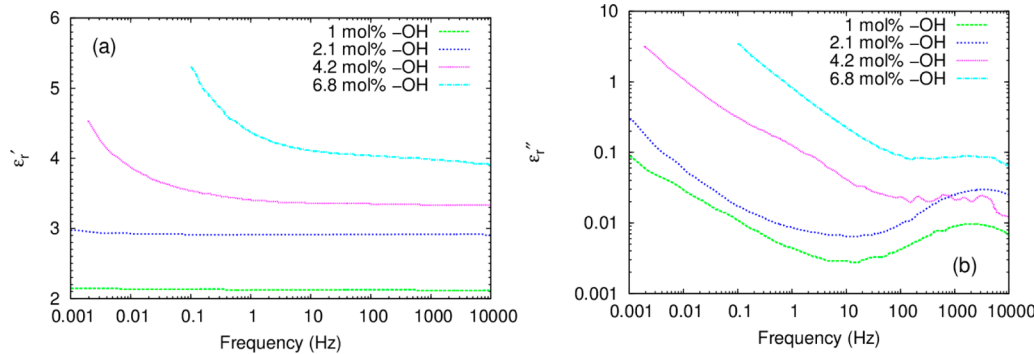
relative permittivity of this dried sample was measured by an HP multifrequency LCR meter in the frequency range of 100 Hz to 1 MHz at room temperature.

In addition to the results for PE–OH, we also present result for PP–OH samples which were described in previous work. The PP–OH results shown in Figure 3 are different from our earlier published results; our previous results corresponded to samples whose water concentrations were not carefully controlled. To drive out water that is not tightly bound to the polymer we stretched the films biaxially and then dried them at 110 °C for 12 h. While we did not characterize the time dependence of the water content, this is a question that we are currently studying. The water content in the samples was measured by differential scanning calorimetry. For a 1.2 mol % –OH sample, it was found to decrease from 1.19 wt % to 0.32 wt % upon drying. Evidently, some fraction of the water is held tenaciously by the polymer, presumably through hydrogen bonds with the –OH groups on the PP chains.

Table 1. Properties of PE and PE-OH Copolymers

run ^a	[OH], ^b mol %	M_v , ^c kDa	T_m , ^d °C	T_c , ^d °C	ΔT , ^d °C	ΔH_m , J/g	χ , ^e %	relative permittivity, 1 kHz	dielectric loss $\times 10^3$, 25 °C, 1 kHz
PE-0	0	2410	134	119	15	142	48	2.29	0.49
PE-3	1.30	1430	129	115	14	136	46	2.87	2.64
PE-4	2.25	1120	128	114	14	115	39	3.06	4.77
PE-7	5.90	1030	128	113	15	81	28	3.89	17.9

^aAl(Et)₂Cl as cocatalyst; the ratio [Al(Et)₂Cl]/[TiCl₃-AA] is 5; polymerized at 70 °C. ^bDetermined by ¹H NMR. ^cDetermined by intrinsic viscosity in decalin at 135 °C with standard of polyethylene. ($M_v = K[\eta]^{\sigma}$, $K = 62 \times 10^{-3}$ mL/g, $\sigma = 0.7$). ^d ΔT was defined as the difference between T_m and T_c . ^eThe crystallinity degree χ was determined by the ratio of ΔH_m to that of a perfect crystal of PE (293.0 J/g).

Figure 4. Frequency dependence of (a) the relative permittivity, ϵ'_r , and (b) the dielectric loss for the PP-OH samples which have been dried.

Our new results (Figure 3) for the static relative permittivity of PP-OH as a function of -OH content are in good agreement with the PE-OH data. The measured static relative permittivity (Table 1, Figure 3) was found to increase with increasing -OH content. These data also follow the same trend as those of PP-OH without the drying step,⁴ but the static relative permittivity measured from the dried samples is systematically lower. While the excess water in PP-OH also apparently increases the relative permittivity without substantially increasing the loss, we consider that the result is likely not stable, so that the water content would reduce to a plateau value with time. Figure 4 shows that the loss for PP-OH remains low except in the very low frequency regime.

3. MOLECULAR DYNAMICS SIMULATIONS

3.1. Simulation Details. In our simulations, we used the optimized potentials for liquid simulations—all atom force field (OPLS-AA). Although many force fields exist for PE, the generic nature of the OPLS-AA formalism lends itself to a wide variety of polymeric systems.¹³ Polarizable force fields could be used for greater accuracy, but we use a nonpolarizable force field due to its computational expediency. Since even the nonpolarizable force field simulations are expensive, we exploit general-purpose graphical processing units (GPGPU) to accelerate the van der Waals and long-range Coulombic calculations,^{14,15} as implemented in LAMMPS.¹⁶

A single polyethylene chain with 1000 backbone carbon atoms was equilibrated at 500 K and 1 bar, where it is in a molten, amorphous state. Samples with 2.2 mol %, 4.2 mol % and 8.2 mol % -OH groups (i.e., 11, 21, and 41 groups per chain, respectively) were prepared using the last configuration of the pure PE simulation run, by directly bonding -OH groups to randomly selected carbons on the polymer backbone, replacing one of the H atoms. (For comparison we bonded the -OH using a C₄H₈ chain as a spacer to the main chain, and these results show the same trends as the main chain functionalized PE.) These -OH contents closely parallel the functionalization levels

realized in both the PE experiments reported here and PP experiments reported previously.⁴ The systems were cooled from 500 to 300 K at 5 K/ns under isobaric conditions. The volume was allowed to stabilize at 300 K for 40–50 ns, followed by 5–6 ns equilibration in the canonical (NVT) ensemble. Thereafter, the net dipole moment was sampled under NVT conditions for 50 ns for calculation of static relative permittivity.

3.2. Crystallinity. Configuration snapshots of PE chains with various levels of -OH content are shown in Figure 5. Visually, crystallinity remains high for the 2.2% and 4.2% samples, but it is significantly decreased for the 8.2% sample. To quantify crystallinity we used a site order parameter. Each carbon is assigned a bond orientation unit vector, which is calculated by connecting the midpoints of its two adjacent backbone bonds.⁷ The bond order parameter between the *i*th atom and the *j*th atom is given by

$$A = \frac{3\langle \cos^2 \varphi \rangle - 1}{2} = \frac{3\langle (\vec{b}_i \cdot \vec{b}_j)^2 \rangle - 1}{2} \quad (1)$$

where \vec{b}_i and \vec{b}_j are unit orientation vectors of the respective atoms. The order parameter for a carbon site is calculated by averaging the bond order parameters for all carbons within a radius of 0.7 nm.¹⁷ A carbon with local order parameter of more than 0.62 ($\varphi = 30^\circ$) was considered crystalline. Using this definition, we find that pure PE was $65 \pm 2\%$ crystalline, while PE-OH samples with 2.2, 4.2, and 8.2 mol % -OH were 56 ± 3 , 57 ± 2 and $32 \pm 2\%$ crystalline, respectively. The trend in crystallinity is qualitatively similar to the PE-OH experimental results (Table 1). The mobility of the polar groups is influenced by the surrounding environment, so we classify each -OH group as belonging to the crystalline, amorphous, or interphase region according to the backbone carbon atom that it is bound to (Table 2). Note that a very high fraction of the -OH groups are in the interphase, probably reflecting Flory's notion that these "defect" groups are rejected from crystal. This segregation gives them

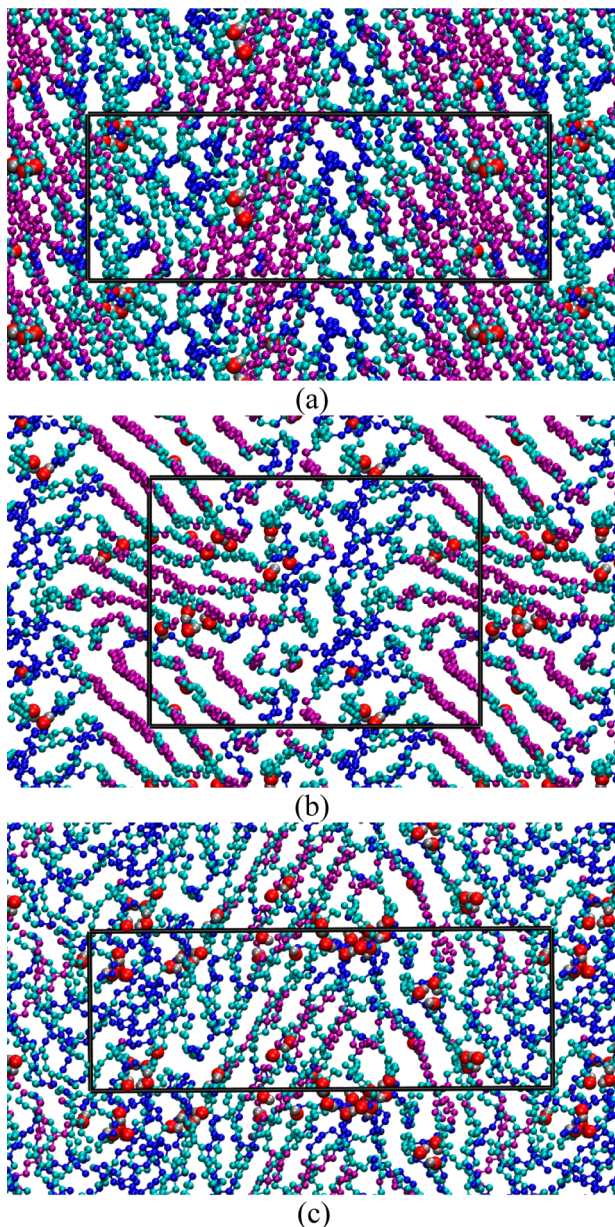


Figure 5. Simulation snapshots of (a) 2.2 mol % PE–OH, (b) 4.2 mol % PE–OH and (c) 8.2 mol % PE–OH. Oxygens and hydroxyl hydrogens are shown as red and silver spheres, respectively. Crystalline, interphase and amorphous carbons are shown in purple, cyan, and blue, respectively. Backbone hydrogens are not shown for clarity. The black box marks the central simulation box of the periodic boundary conditions.

Table 2. Fraction of –OH Groups in the Amorphous, Crystalline, and Interphase Regions^a

	amorphous	crystalline	interphase
2.2	0.12	0.01	0.87
4.2	0.14	0.10	0.76
8.2	0.26	0.02	0.72

^aA carbon with local order parameter of more than 0.62 ($\varphi = 30^\circ$) was considered crystalline, less than −0.12 ($\varphi = 60^\circ$) was considered amorphous, and interphase otherwise.

more mobility for reorientation, which increases the static relative permittivity.

3.3. Static Relative Permittivity. The static relative permittivity is computed as^{18,19}

$$\epsilon_{\text{rel}} = \epsilon_{\infty} + \frac{4\pi\langle M^2 \rangle}{3Vk_B T} \quad (2)$$

where M is the dipole moment of the simulation box, k_B is Boltzmann's constant, T is the temperature, and V is the simulation volume, and the constant $\epsilon_{\infty} = 2.2$ accounts for the electronic component not included in the classical MD calculations. The calculated ϵ_{rel} , shown in Table 3, is in good agreement with the value obtained from experiments (Figure 3).

Table 3. Dipole Moment and Static Relative Permittivity for PE–OH System with Varying Amounts of –OH

mol % H ₂ O	$\langle M^2 \rangle$	$\langle M \rangle^2$	$\langle M \rangle^2/\langle M^2 \rangle$	ϵ_{rel}
2.2	0.49	0.14	0.29	2.71
4.2	1.23	0.45	0.37	3.53
8.2	2.08	1.18	0.57	4.42

However, the system was found to have a remnant dipole moment, $\langle M \rangle$, over the simulation time scale of 100 ns. In particular, this unrelaxed part at 100 ns for 2.2, 4.2, and 8.2 mol % –OH was found to be 29%, 37% and 57%, respectively, expressed as the ratio $\langle M \rangle^2/\langle M^2 \rangle$ (Table 3). Two salient points are emphasized here. First, for melts of PE–OH at $T = 500$ K, $\langle M \rangle$ relaxes to zero over this simulation time scale. Second, a detailed examination of our simulations shows that the –OH groups that are accidentally incorporated in the crystal domains relax over time scales shorter than 100 ns. Thus, this unrelaxed dipole moment is not due to constraints from the crystal. Rather, we conjecture that they are from hydrogen bonding interactions that do not decay over the 100 ns time scales accessible in the simulations. A corollary to this statement is that the relaxations of these H-bonded interactions should give rise to large dielectric losses at time scales longer than 100 ns. Since our experiments (Table 1) show low dielectric loss, some other phenomenon is at play here. In particular, we conjecture that these differences are caused by the presence of the small amount of “bound” water in both the PE–OH and PP–OH samples.

To examine the presence of water, we chose the 4.2 mol % PE–OH system for further study, to which we added varying amounts of water in a series of simulations. The water molecules were described by the transferable intermolecular four-point potential (TIP4P) model,²⁰ and were added randomly to the last configuration of the 4.2 mol % PE–OH simulation at 300 K. Each system was heated to 500 K and then cooled to 300 K using the same protocol as for the dry PE–OH simulations. The addition of water causes a significant increase in ϵ_{rel} , which overpredicts the experiments (Figure 6). The definition of ϵ_{rel} (eq 2) assumes that the net dipole moment relaxes completely at long time, but there exists another quantity,²¹

$$\tilde{\epsilon}_{\text{rel}} = \epsilon_{\infty} + \frac{4\pi(\langle M^2 \rangle - \langle M \rangle^2)}{3Vk_B T} \quad (3)$$

whose latent assumption is that the remnant dipole moment never relaxes and thus does not contribute to the static relative permittivity. This assumption is compatible with the experimental observation that these materials have low loss in the experimental time scale. This curve for $\tilde{\epsilon}_{\text{rel}}$ (eq 3) is also plotted in Figure 6, and is systematically lower than that for ϵ_{rel} . We note that there exists a finite water content at which $\tilde{\epsilon}_{\text{rel}}$ agrees with

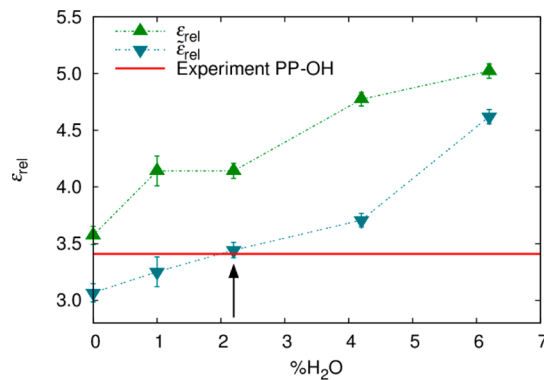


Figure 6. Static relative permittivity for 4.2 mol % PE–OH as a function of added water, calculated using two different methods. Green triangles are ϵ_{rel} (eq 2), while blue inverted triangles are $\bar{\epsilon}_{\text{rel}}$ (eq3). The red line represents the static relative permittivity measured for the 4.2 mol % PP–OH. The arrow marks the plateau water concentration computed by simulations (section 3.4).

experiment, but the actual water content must be characterized to establish this point of agreement.

3.4. Water Content. We consider two ways to characterize the water content from the simulations. First, we pursue an analysis based on hydrogen bonding. Later, a more extensive calculation based on dielectric loss will support the same conclusions. A key to the analysis is the distinction between free and bound water. We consider a water molecule to be bound if it is connected to a hydroxyl group by at least one hydrogen bond and free otherwise. Hydrogen bonds are defined according to the standard procedure, with a cutoff distance of 0.3 nm and a cutoff angle of 30° .^{23,24} We find that the amount of bound water increases with increasing water content, up to ~ 2.2 mol %, beyond which this bound population reaches a plateau, while the free population continues to grow (Figure 7). We therefore

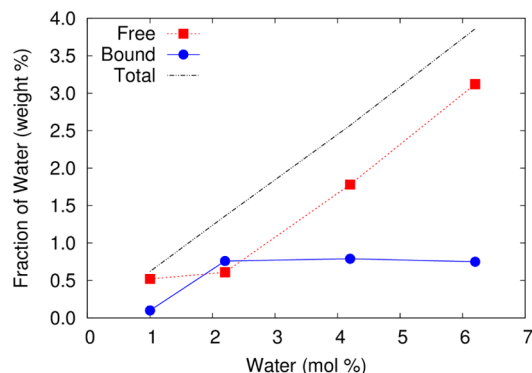


Figure 7. Weight percentage of free, bound, and total water in the system as a function of water in the 4.2 mol % PE–OH. Error bars are smaller than the symbol size.

conclude that all additional water molecules beyond this plateau join the population of free water, and we expect that further addition of water will eventually lead to macroscopic phase separation between a pure water phase and a PE–OH phase with adsorbed water. We define the plateau concentration of 2.2 mol % as the equilibrium water content in this sample. This concentration corresponds to a ratio of ~ 0.5 water molecules per hydroxyl group, which is in good agreement with the experimental measurements discussed in section 2.2, where the 0.32 wt % water content in the 1.2 mol % –OH sample

corresponds to a ratio of 0.41 H₂O/–OH. The plateau concentration also identifies the point at which $\bar{\epsilon}_{\text{rel}}$ agrees with experiment (Figure 6, see arrow). The implications of this agreement will be addressed in the Discussion.

3.5. Dielectric Loss. In the previous section, the fluctuation of the system dipole moment was used to calculate the static relative permittivity. Here, we use the related autocorrelation function to calculate the dielectric loss as a function of frequency, but we can only access frequencies within the time scale of the simulation. We calculate the dielectric decay function (DDF)¹⁹

$$\Phi(t) = \frac{\langle \vec{M}(0) \cdot \vec{M}(t) \rangle - \langle \vec{M}(0) \rangle^2}{\langle M^2 \rangle - \langle M \rangle^2} \quad (4)$$

where $\vec{M}(t)$ is the dipole moment at time t (Figure 8), which we fit with a stretched exponential form with a prefactor: $\Phi_{\text{fit}}(t) = A \exp[-(t/\tau)^\alpha]$. The prefactor represents a very fast initial decay of strength $1 - A$.

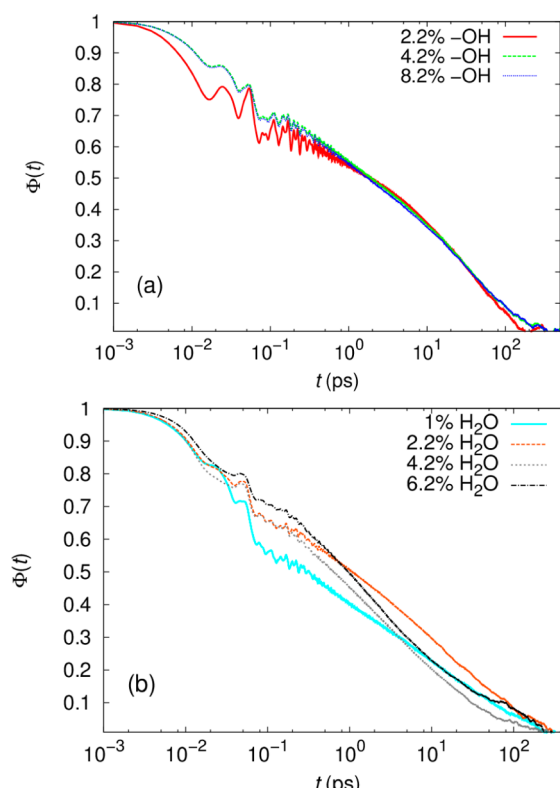


Figure 8. Dielectric decay function for (a) PE–OH systems with varying –OH concentrations and (b) 4.2 mol % PE–OH system with varying water content.

The fitted function (Table 4) was Fourier-transformed to calculate the complex dielectric permittivity, $\epsilon^*(\omega) = \epsilon'(\omega) - i\epsilon''(\omega)$ ¹⁹

$$\frac{\epsilon^*(\omega)}{\Delta\epsilon} = \int_0^\infty e^{i\omega t} \frac{d\Phi_{\text{fit}}(t)}{dt} dt \quad (5)$$

whose imaginary part is the dielectric loss (Figure 9). The average relaxation time was calculated as $\tau_{\text{avg}} = 1/\omega_{\text{max}}$ ²² where ω_{max} is the angular frequency of the peak $\epsilon''(\omega)$.

In the dry PE–OH system we observed that the relaxation time remains constant while the dielectric loss increases with increasing –OH content. The addition of 1.0 mol % water to the 4.2 mol % PE–OH system decreased the relaxation time from 27

Table 4. Mean Relaxation Time and Fitting Parameter for Dielectric Decay Function Using Stretched Exponential Form for PE–OH Systems with Varying –OH and Water Concentrations

mol % –OH	A	τ (ps)	α	ϵ''_{\max}	ω_{\max} (Hz)	τ_{avg} (ps)
2.2	0.64	26	0.57	0.08	3.0×10^{10}	33
4.2	0.73	20	0.45	0.16	3.7×10^{10}	27
8.2	0.73	19	0.44	0.18	3.8×10^{10}	26
mol % H ₂ O	A	τ (ps)	α	ϵ''_{\max}	ω_{\max} (Hz)	τ_{avg} (ps)
1	0.66	8.1	0.35	0.14	8.3×10^{10}	12
2.2	0.75	14	0.37	0.20	4.9×10^{10}	20
4.2	0.89	2.8	0.33	0.27	2.4×10^{11}	4.2
6.2	1.0	1.3	0.25	0.44	4.8×10^{11}	2.1

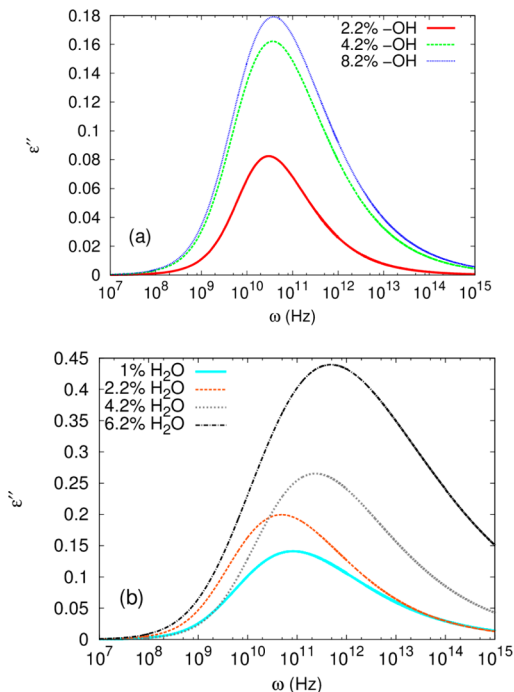


Figure 9. Dielectric loss ϵ'' for (a) PE–OH systems with varying –OH concentrations and (b) 4.2 mol % PE–OH system with varying water content.

to 12 ps. The relaxation time increased for the 2.2% H₂O system, and then decreased for systems with higher water content. This was also accompanied by a decrease in the prefactor A, which suggests that the very fast relaxation process becomes less important with increasing water content. A similar non-monotonic behavior of relaxation time was observed in simulations of polyoxyethylene diluted by water,¹⁹ and this behavior was attributed to different relaxation behavior between free water and water bound to the polymer and to their changing relative populations with increasing water content.

To further explore the influence of water on the relaxation, we measured the dipole moment of the water molecules only and calculated their dielectric decay function (Figure 10). We find that this DDF can be fit with sum of two stretched exponential functions:

$$\Phi_{\text{fit}}(t) = A \exp\left[-\left(\frac{t}{\tau_1}\right)^{\alpha_1}\right] + (1 - A) \exp\left[-\left(\frac{t}{\tau_2}\right)^{\alpha_2}\right] \quad (6)$$

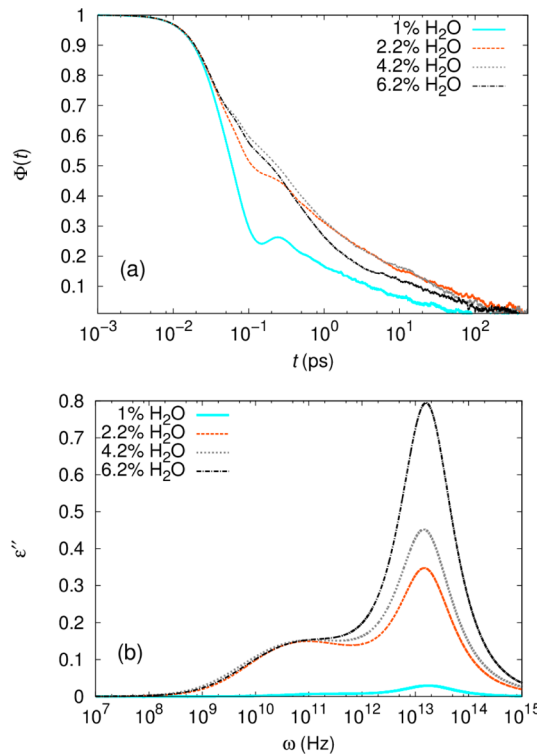


Figure 10. (a) Dielectric decay function $\Phi(t)$, and (b) dielectric loss ϵ'' for water in 4.2 mol % PE–OH system with varying water content.

After the Fourier transform to find ϵ'' , two peaks appear, at ~ 12 and ~ 0.06 ps (Table 5), which are in agreement with the two different water relaxation peaks identified measurements of organic materials.²⁵ Both relaxation times obtained are much faster than the relaxation time of 4.2 mol % PE–OH sample without water (27 ps), which suggests that water accelerates the relaxation dynamics of the system. The height of the higher frequency peak increases with increasing water content, which we identify as the free water peak. In contrast, the lower frequency peak saturates at 2.2%, which is in perfect agreement with the behavior of the bound water fraction as found through the less computationally intensive, static hydrogen-bond analysis. The bound water peak not only has a longer relaxation time but also has wider tail, due to lower α_1 (Table 5), which gives rise to increased loss at lower frequency, although the loss implied is still negligible for frequencies less than 1 MHz. Though the free water has a higher loss peak, its relaxation both occurs at a higher frequency and decays more quickly with frequency, since $\alpha_2 = 1$, which corresponds to a Debye process. These imply that additional free water will increase the static relative permittivity without increasing loss below 1 MHz, which is what experiments observed.

4. DISCUSSION

To summarize, we have found several points of agreement between the simulations of PE–OH with water and the experiments. The static relative permittivity, $\tilde{\epsilon}_{\text{rel}}$ and the stoichiometric ratio of water molecules to hydroxyl groups match experiments (section 3.3). Additionally, the dielectric loss analysis of the water molecules explains how additional water increases the static relative permittivity without adding loss in the experimental measurement (section 3.5). Finally, the good agreement between the static relative permittivity $\tilde{\epsilon}_{\text{rel}}$ (eq 3) and experiment, combined with the formula's built-in assumptions—

Table 5. Mean Relaxation Time and Fitting Parameter for Dielectric Decay Function for Water in 4.2 mol % PE–OH System with Varying Water Content

mol % H ₂ O	A	τ_1 (ps)	α_1	τ_2 (fs)	α_2	$\omega_{1,\max}$ (Hz)	$\omega_{2,\max}$ (Hz)	$\tau_{1,\text{avg}}$ (ps)	$\tau_{2,\text{avg}}$ (fs)
1	0.30	3.7	0.50	56	1.0	2.0×10^{11}	1.8×10^{13}	5.0	56
2.2	0.53	8.5	0.39	65	1.0	8.1×10^{10}	1.5×10^{13}	12	67
4.2	0.49	11	0.35	87	1.0	6.2×10^{10}	1.2×10^{13}	16	83
6.2	0.32	12	0.36	99	1.0	5.3×10^{10}	1.0×10^{13}	19	100

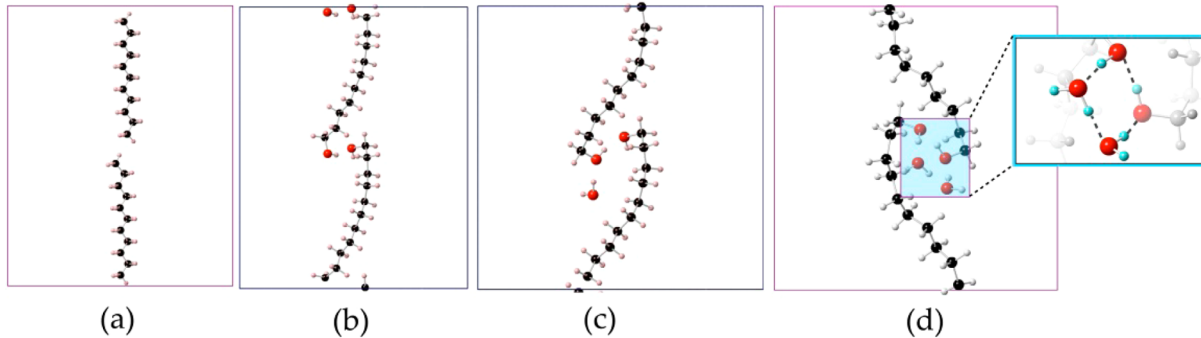


Figure 11. Optimized structures of (a) o-PE, (b) o-PE–OH, (c) o-PE–OH–H₂O, and (d) o-PE–OH–2H₂O. Black, white, and red spheres represent C, H, and O atoms, respectively. The inset shows a typical hydrogen bonded ring (H atoms are cyan).

that the dipole moment that does not relax on simulation time scales also does not contribute to the relative permittivity—imply that there should be low loss in the experiments, which do find the loss to be quite low.

However, we also found striking agreement in the relative permittivity between the simulations with dry PE–OH and the experiments under a different set of assumptions, namely that the system relaxes completely, so that the entire variance of the dipole moment contributes to the static relative permittivity (Figure 3). Although the experimental samples are known to contain a small amount of adsorbed water (that was not included in the dry PE–OH simulations), we argue that the agreement seen in Figure 3 is not coincidental. Specifically, we argue that the simulations are an accurate representation of what would be measured if the experimental samples could be made without any adsorbed water. This is an unproven conjecture, that remains to be verified by experiment. If this is true, it implies that hydrogen-bonded –OH groups will relax within the experimental time scale, but when they are bridged by water, they become more strongly constrained and do not relax. Thus dry PE–OH should be very lossy while wet PE–OH is not.

Supporting evidence in favor of this conjecture can be found by analyzing the amount of relaxation that occurs within the simulation time scale. For the 4.2 mol % PE–OH system with 2.2 mol % water, we separately analyzed the dipole autocorrelation of each CH–OH group (as a net neutral group of atoms), and we found that 69% of the groups were bound to one another via a bridging water molecule, while the other 31% were either single or H-bonded directly to another –OH group. We find that those bridged by water relaxed the least while those not water-bridged relaxed the most; the Pearson correlation coefficient relating water bridging to relaxation is -0.73 suggesting a strong anticorrelation. Quantified another way, 89% of the remnant dipole at 100 ns is due to water-bridged hydroxyl groups. The water in these groups are tightly bound, having a loss peak about 2 orders of magnitude smaller in frequency than free water.

In molecular dynamics simulations, we observed clusters of two or three hydroxyl groups and associated water molecules held together by hydrogen bonds in highly geometrically

constrained structures. We also used DFT with a much smaller system to demonstrate that these clusters also form with an *ab initio* method. We used the Vienna *ab initio* simulation package (VASP),²⁶ with projector-augmented wave frozen-core potentials^{27,28} to represent the valence electrons, and the Perdew–Burke–Ernzerhof functional with the Grimme D2 correction (PBE-D2) was used to handle the van der Waals (vdW) interactions.^{29,30} Since vdW interactions were accounted for,^{31,32} the computation captures secondary bonding phenomena such as H-bonding. We simulated four systems. All started with two 11-carbon PE oligomers (o-PE), initially arranged head-to-tail. In three systems, we substituted a hydroxyl group in place of a hydrogen atom at each end of both chains (o-PE–OH). For two others, we added additional one or two water molecules, (o-PE–OH–H₂O and o-PE–OH–2H₂O, respectively). For all systems, we found the optimized geometries (Figure 11). Hydrogen bonding is apparent in these configurations, especially in Figure 11d, where a hydrogen-bonded ring of two hydroxyl groups and two water molecules is clearly evident.

5. SUMMARY

Inspired by previous experimental results for PP–OH,⁴ we conducted experiments and simulations to study the dielectric properties of PE–OH and performed new measurements of PP–OH where the excess water was driven out. The experiments show that PP–OH and PE–OH are essentially equivalent in dielectric properties. The static relative permittivity from simulations of dry PE–OH was in relatively good agreement with the experiments, but the result implies high loss in the experimental time scale. Since this is inconsistent with experiment, we conjecture that some other phenomenon is relevant.

Simulations of PE–OH with added water both predict the plateau water content, which was corroborated by experiments, and predict the static relative permittivity of this system, which agreed quantitatively with the experimental result, after taking into account the experimental observation that loss is low over the experimental time scale. Dielectric loss calculations showed that the water in the system relaxes in the simulation time scale of

100 ns and that there are two populations of water: free water that relaxes quickly and bound water that relaxes 100 times more slowly. These results together suggest that the mechanistic reason that PE-OH and PP-OH can have both increased relative permittivity and low loss is that there is a stoichiometric amount of adsorbed water that forms tightly H-bonded clusters of water molecules and hydroxyl groups. These clusters prevent the -OH groups from relaxing and contributing to the dielectric loss, except possibly at time scales longer than the experimental measurement.

■ ASSOCIATED CONTENT

Supporting Information

Polymerization procedures and ^1H NMR spectrum, TGA results, and DSC curves of copolymer PE-7. This material is available free of charge via the Internet at <http://pubs.acs.org>.

■ AUTHOR INFORMATION

Corresponding Author

*(S.K.K.) E-mail: sk2794@columbia.edu.

Notes

The authors declare no competing financial interest.

■ ACKNOWLEDGMENTS

The authors gratefully acknowledge financial support for this work through a Multidisciplinary University Research Initiative (MURI) grant from the Office of Naval Research under Contract No. N00014-99-1-0443. The simulations presented in this paper were performed on computational resources supported by the National Energy Research Scientific Computing Center, which is supported by the Office of Science of the U.S. Department of Energy under Contract No. DE-AC02-05CH11231.

■ REFERENCES

- (1) Ho, J.; Ramprasad, R.; Boggs, S. *IEEE Trans. Dielectr. Electr. Insul.* **2007**, *14*, 1295–1301.
- (2) Boggs, S. *IEEE Electr. Insul. Mag.* **2010**, *26*, 8–22.
- (3) Boggs, S.; Ho, J.; Jow, T. *IEEE Electr. Insul. Mag.* **2010**, *26*, 7–13.
- (4) Yuan, X.; Matsuyama, Y.; Chung, T. C. M. *Macromolecules* **2010**, *43*, 4011–4015.
- (5) Yamamoto, T.; Sawada, K. *J. Chem. Phys.* **2005**, *123*, 234906.
- (6) Liu, C.; Muthukumar, M. *J. Chem. Phys.* **1998**, *109*, 2536.
- (7) Fujiwara, S.; Sato, T. *J. Chem. Phys.* **1997**, *107*, 613.
- (8) Welch, P.; Muthukumar, M. *Phys. Rev. Lett.* **2001**, *87*, 218302.
- (9) Yamamoto, T. *Polymer* **2009**, *50*, 1975–1985.
- (10) Yi, P.; Rutledge, G. C. *J. Chem. Phys.* **2009**, *131*, 134902.
- (11) Gee, R. H.; Lacevic, N.; Fried, L. E. *Nat. Mater.* **2006**, *5*, 39–43.
- (12) Ramos, J.; Martínez-Salazar, J. *J. Polym. Sci., Part B: Polym. Phys.* **2011**, *49*, 421–430.
- (13) Jorgensen, W. L.; Maxwell, D. S.; Tirado-Rives, J. *J. Am. Chem. Soc.* **1996**, *118*, 11225–11236.
- (14) Stone, J. E.; Phillips, J. C.; Freddolino, P. L.; Hardy, D. J.; Trabuco, L. G.; Schulten, K. *J. Comput. Chem.* **2007**, *28*, 2618–40.
- (15) Anderson, J. A.; Lorenz, C. D.; Travesset, A. *J. Comput. Phys.* **2008**, *227*, 5342–5359.
- (16) Plimpton, S. *J. Comput. Phys.* **1995**, *117*, 1–19.
- (17) Yu, X.; Kong, B.; Yang, X. *Macromolecules* **2008**, *41*, 6733–6740.
- (18) Fröhlich, H.; Maradudin, A. *Theory of Dielectrics*, 2nd ed.; Oxford University Press: Oxford, U.K., 1958; Vol. 12, p 192.
- (19) Borodin, O.; Bedrov, D.; Smith, G. D. *Macromolecules* **2002**, *35*, 2410–2412.
- (20) Jorgensen, W. L.; Chandrasekhar, J.; Madura, J. D.; Impey, R. W.; Klein, M. L. *J. Chem. Phys.* **1983**, *79*, 926.
- (21) Karasawa, N.; Goddard, W. A. *Macromolecules* **1995**, *28*, 6765–6772.
- (22) Alvarez, F.; Alegra, A.; Colmenero, J. *Phys. Rev. B* **1991**, *44*, 7306–7312.
- (23) Noskov, S. Y.; Lamoureux, G.; Roux, B. *J. Phys. Chem. B* **2005**, *109*, 6705–13.
- (24) Provencal, R. A.; Casaes, R. N.; Roth, K.; Paul, J. B.; Chapo, C. N.; Saykally, R. J.; Tschumper, G. S.; Schaefer, H. F. *J. Phys. Chem. A* **2000**, *104*, 1423–1429.
- (25) Buchner, R.; Barthel, J.; Stauber, J. *Chem. Phys. Lett.* **1999**, *306*, 57–63.
- (26) Kresse, G.; Joubert, D. *Phys. Rev. B* **1999**, *59*, 11–19.
- (27) Kresse, G.; Furthmüller, J. *Phys. Rev. B. Condens. Matter* **1996**, *54*, 11169–11186.
- (28) Blöchl, P. *Phys. Rev. B* **1994**, *50*, 17953–17979.
- (29) Langreth, D. C.; Dion, M.; Rydberg, H.; Schröder, E.; Hyldgaard, P.; Lundqvist, B. I. *Int. J. Quantum Chem.* **2005**, *101*, 599–610.
- (30) Grimme, S. *J. Comput. Chem.* **2006**, *27*, 1787–1799.
- (31) Liu, C.-S.; Pilania, G.; Wang, C.; Ramprasad, R. *J. Phys. Chem. A* **2012**, *116*, 9347–52.
- (32) Pilania, G.; Ramprasad, R. *J. Mater. Sci.* **2012**, *47*, 7580–7586.